

Fig. 1. Basic configuration, wideband coaxial-line power divider.

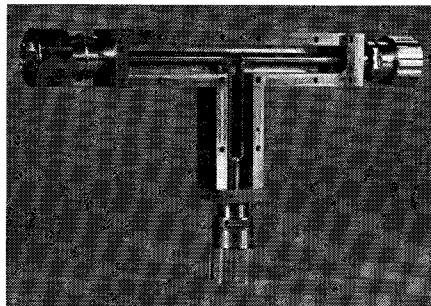


Fig. 2. Internal view, wideband coaxial-line power divider.

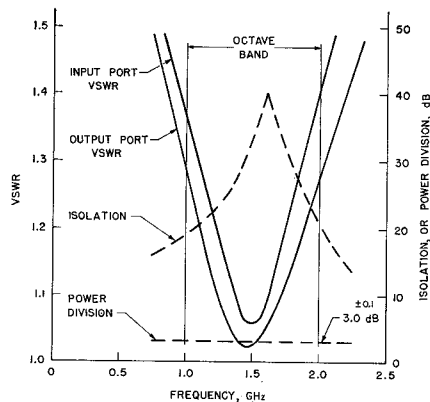


Fig. 3. Performance, wideband coaxial-line power divider.

bandwidth of the power divider; it is directly observed as a reduction in the output-port reflection and as an increase in the isolation between the output ports. It is noted that the output-port reflection is a phasor combination of the sum port reflection and the (inaccessible) difference port reflection.

Figure 3 presents the measured performance of the wideband power divider. Over the octave band from 1.0 to 2.0 GHz, the VSWR at any port is less than 1.4 (3.0 dB SWR), the isolation between output ports is greater than 19 dB and the power division is equal to 3.0 dB. More details on the development and performance may be found in a previous report.<sup>3</sup>

It is estimated the wideband power divider design with reactive compensation of the dif-

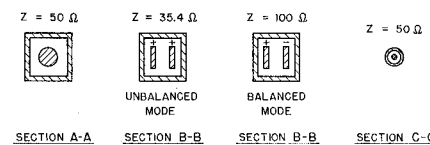


Fig. 1. Basic configuration, wideband coaxial-line power divider.

ference port reflection provides at least a 2 to 1 increase in bandwidth over a comparable uncompensated design. An even further increase in the bandwidth of this type of power divider is possible. It would be obtained by 1) reactive compensation of the sum port reflection by a parallel, open-circuited quarter-wavelength stub located in the input coaxial line one quarter wavelength from the junction, and 2) adjusting the reactive compensation of the difference port reflection to obtain an edge-band match as distinguished from the mid-band match used here.

#### ACKNOWLEDGMENT

The author would like to express thanks to W. K. Kahn who was the report advisor; and to H. A. Wheeler who provided guidance and general direction.

SIDNEY DAVID  
Wheeler Laboratories, Inc.  
Great Neck, N. Y.

#### Octave Bandwidth L- and S-Band Stripline Discriminators

The purpose of this correspondence is to describe the design details and measured characteristics of two octave bandwidth stripline discriminators for L- and S-bands. The discriminators are constructed with the schematic arrangement described by Mohr<sup>1</sup> using two 3 dB wideband directional couplers with an additional  $3\lambda/4$  line (at the center frequency) in one of the branches. Mohr's correspondence, though briefly describing the experimental results on an L-band coaxial line discriminator, does not give design details of the unit. In the Mohr arrangement the powers coupled to ports 2 and 3 (see Fig. 1) have the ratio,

$$\frac{P_2}{P_3} = \frac{\frac{1}{2}P_i[1 - \cos \Phi]}{\frac{1}{2}P_i[1 + \cos \Phi]} = \tan^2 \frac{\Phi}{2}$$

where  $\Phi$  is the frequency dependent phase difference of the additional length  $l$  in the line between ports  $P_1$  and  $P_2$  ( $= 2\pi l/\lambda$ ).

Manuscript received September 1, 1966; revised October 19, 1966.

<sup>1</sup> R. J. Mohr, "Broad-band microwave discriminator," *IEEE Trans. on Microwave Theory and Techniques (Correspondence)*, vol. MTT-11, pp. 263-264, July 1963.

It is necessary, for the above relationship to hold true, that the phase shift between the 3 dB down coupled component and equal transmitted component, be 90 degrees regardless of the frequency, which is true only for symmetric-line directional couplers, hence these are used in this construction. For slight asymmetry in the coupled lines, however, the phase shift between the two components is different from 90 degrees by a small amount  $\theta$  which is a function of the frequency. In such a case the aforementioned relationship for  $P_2/P_3$  gets modified to  $\tan^2(\Phi/2 + \theta)$  assuming of course, that the same amount of asymmetry exists in both the 3 dB hybrids used in the discriminator. The schematic arrangement for the two lines is shown in Fig. 1. Each of the 3 dB hybrids  $A$  and  $B$  consists of three sections with broadside coupling<sup>2</sup> for the central section (coupling coefficient = 0.8273) and coplanar coupling<sup>3</sup> for the two outer sections (coupling coefficient = 0.1550). The three section symmetrical couplers were used in preference to single sections to reduce the coupling variation over the octave frequency bandwidth. The coupling variation of the three section hybrids used in this construction was, in fact, separately measured to be  $-3 \pm 0.3$  dB over the 0.9-2.0 GHz band for the L-band unit, thus proving the validity of their design for wide bandwidth operation. For the S-band hybrid the length of the three coupled sections is exactly halved with the stripline widths and the interline spacings maintained same as those in the L-band hybrid. For the central section the coupling coefficient of 0.8273 being very large, it was not possible to obtain this by means of coplanar coupled lines and hence broadside coupled central section was used. The striplines from ports  $P_1$  to  $P_2$  and  $P_3$  to  $P_4$  (shown dotted) are printed on individual copper-clad boards which are then placed facing each other. For the broadside coupled section the lines are separated by a 0.008 inch thick teflon strip (shown dotted at  $S_1$  and  $S_2$ ) as against the design value of 0.013 inch, for experimentally obtained optimum performance of the hybrids and of the discriminator units. The  $3\lambda/4$  line (at the center frequency) is provided by the additional length 1 inch stripline  $P_1P_2$ .

The measured results on the L- and S-band units are shown in Figs. 2, 3, and 4. The experimental values of power discrimination are as high as 15-18 dB at the frequency ends. The power ratio  $P_2/P_3$  is plotted in Figs. 2 and 3 and compared with theoretical variation  $20 \log \tan \Phi/2$ . The discrepancy in  $P_2/P_3$  between the theoretical and experimental results is ascribed to the slight asymmetry in the hybrids as a result of the not-so-loosely coupled sections  $C_1$  and  $C_2$  and a probable misalignment in the placement of the two boards. The additional phase shift  $\theta$  thus produced is calculated from the comparison of experimental and theoretical data and is listed in Table I.

The VSWR over the octave bandwidth for

<sup>2</sup> S. B. Cohn, "Characteristic impedances of broadside-coupled strip transmission lines," *IEEE Trans. on Microwave Theory and Techniques*, vol. MTT-9, pp. 633-637, November 1960.

<sup>3</sup> S. B. Cohn, "Shielded coupled-strip transmission line," *IEEE Trans. on Microwave Theory and Techniques*, vol. MTT-3, pp. 29-38, October 1955.

<sup>3</sup> S. David, "A wideband coaxial-line power divider," M.S.E. rept., Polytechnic Inst. of Brooklyn, Brooklyn, N. Y., 1966.

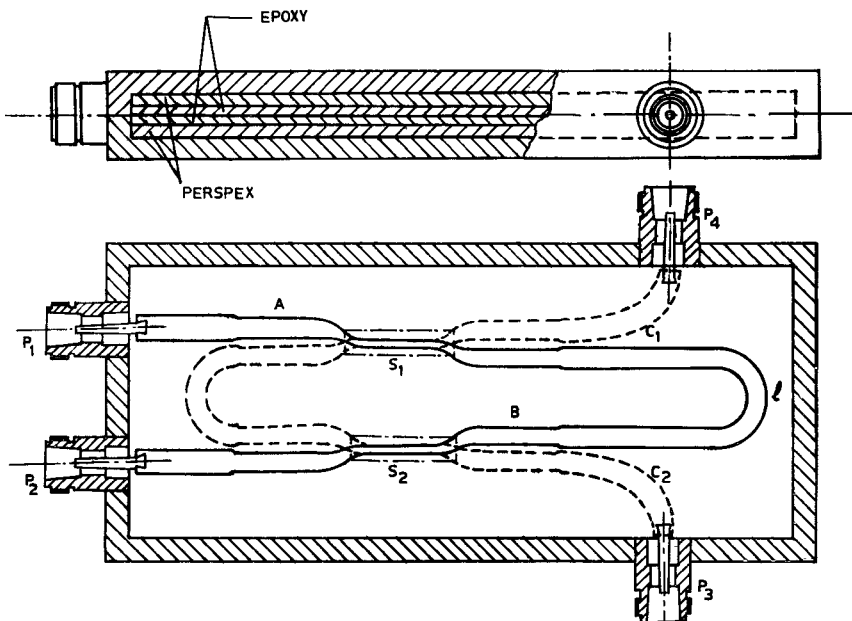


Fig. 1. Schematic layout of the discriminator (dotted stripline printed on separate board).

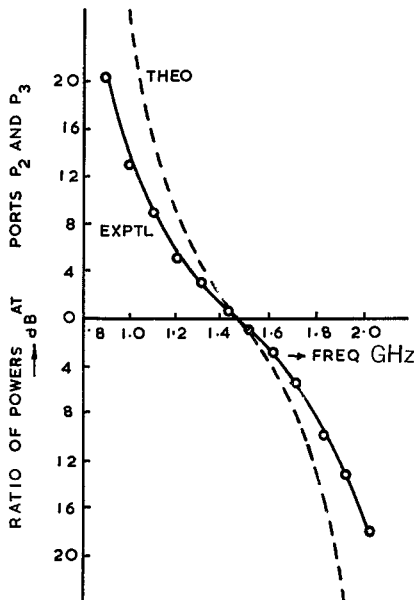


Fig. 2. Power discrimination characteristic of the L-band discriminator.

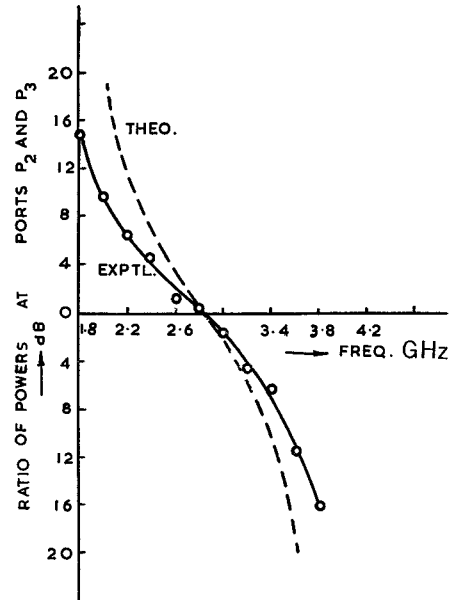


Fig. 3. Power discrimination characteristic of the S-band discriminator.

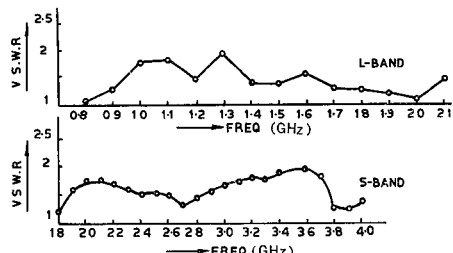


Fig. 4. VSWR characteristics of the L- and S-band discriminators.

the two units is less than 2.0, as shown in Fig. 4. The VSWR is somewhat higher than in normal stripline components on account of several relatively sharp changes in the stripline locations. The discrimination at the frequency ends is consequently reduced on this account and also due to the fact that epoxy board rather than teflon impregnated fiberglass board was used for printed striplines on account of the unavailability of the latter and this material is known to be more lossy at microwave frequencies. The discrimination is, however, adequate for usual discriminator applications. The power at the uncoupled port  $P_4$ , in each of the units is more than 15 dB (mostly larger than 20 dB for L-band unit) below the incident power over the frequency band of operation.

#### ACKNOWLEDGMENT

The authors gratefully acknowledge the work of V. P. Bhatnagar on the L-band discriminator.

M. L. SISODIA  
O. P. GANDHI  
Central Electronics  
Engrg. Research Inst.  
Pilani (Rajasthan), India

#### High-Q Microwave Filters Employing IMPATT Active Elements

During the course of switching studies<sup>1</sup> an unusually large transmission on/off ratio was obtained from an X-band single PIN diode switch operating in the milliwatt range. The phenomenon is attributed to the generation of a microwave negative resistance of the IMPATT type (*Impact Avalanche Transit Time*) when reverse bias current flows. This negative resistance cancels the normal series  $R_S$  loss of the diode and associated contact losses giving a true wideband zero loss waveguide switch.

Figure 1 shows the lumped element equivalent circuit. Under forward bias the total diode impedance ( $Z$ ) approximates a short circuit with the package capacity ( $C_p$ ) and the contacting spring ( $L_s$ ) in parallel resonance creating a bandpass circuit. When the diode is appreciably reverse biased (but not into breakdown) the diode impedance becomes a large capacitive reactance allowing the inductive stub and the package capacity to be series resonant. Figure 2 shows the typical "off" transmission characteristics. The dotted transmission loss characteristic of Fig. 2 represents the maximum possible loss for this circuit with passive elements found experimentally by replacing the encapsulated diode with an open circuit package. When 2 mA of reverse current is drawn, the transmission loss jumps to 55 dB as shown in Fig. 3, an increase

TABLE I

L-Band Unit		S-Band Unit	
Frequency GHz	$\theta$ Radians	Frequency GHz	$\theta$ Radians
1.0	0.1386	2.0	0.2287
1.1	0.1638	2.2	0.1944
1.2	0.1275	2.4	0.1104
1.3	0.0466	2.6	0.1384
1.4	0.0256	2.8	0.0286
1.5	-0.044	3.0	-0.0371
1.6	-0.1339	3.2	-0.0417
1.7	-0.1364	3.4	-0.1374
1.8	-0.1217	3.6	-0.1204
1.9	-0.1987	3.8	-0.1034

Manuscript received September 21, 1966.

<sup>1</sup> R. W. Dawson and B. C. De Loach, "A low loss 1 nanosecond 1 watt X-band switch," *Symp. D'gest—Internat'l Symp. on Microwave Theory and Techniques*, 1966.